NJC

Accepted Manuscript

This article can be cited before page numbers have been issued, to do this please use: N. E. Aksakal, H. H. KAZAN, E. Tanrverdi Eçik and F. Yuksel, *New J. Chem.*, 2018, DOI: 10.1039/C8NJ02944J.

ROYAL SOCIETY OF CHEMISTRY

rsc.li/njc

View Article Online
DOI: 10.1039/C8NJ02944J

A novel photosensitizer based on a ruthenium(II) phenanthroline bis(perylenediimide) dyad: synthesis, generation of singlet oxygen and *in vitro* photodynamic therapy

Nuray Esra Aksakal[a], Hasan Hüseyin Kazan[b], Esra Tanrıverdi Eçik[a], Fatma Yuksel[a]*

[a] Department of Chemistry, Faculty of Science, Gebze Technical University, Gebze, Kocaeli, Turkey

[b] Department of Biological Sciences, Middle East Technical University, Ankara, Turkey

* Author for correspondence:

Prof. Dr. Fatma Yuksel, Department of Chemistry, Gebze Technical University, P.O.Box: 141, Gebze 41400, Kocaeli, Turkey

Tel: 00 90 262 6053016

Fax: 00 90 262 6053005

e-mail : fatma@gtu.edu.tr

KEYWORDS: Ruthenium(II) complex, Perylene diimide, Photodynamic Therapy, Singlet Oxygen, Leukemia cells

View Article Online
DOI: 10.1039/C8NJ02944J

ABSTRACT

In this study, a novel photosensitizer having two perylenediimide and phenanthroline ruthenium (II) coordination moieties (**Ru-BP**) has been developed for photodynamic therapy (PDT) of cancer cells. This new compound was prepared *via* reaction of two newly designed molecules, namely 5,6,12,13-tetrakis(4-(tert-butyl)phenoxy)-2-(2,6-diisopropylphenyl)-9-(4-hydroxyphenyl)anthra[2,1,9-def:6,5,10-d'e'f']diisoquinoline-1,3,8,10(2H,9H)-tetraone (**P6**) and bis(2,2'-bipyridyl)-(4,7-dichlorophenanthroline)ruthenium(II) complex (**7**). The singlet oxygen productions of **P6** and **Ru-BP** were investigated by chemical method using trap molecule as 1,3-diphenylisobenzofurane. Additionally, photodynamic therapy efficacy of the novel **Ru-BP** complex and **P6** were evaluated *in vitro*. **Ru-BP** significantly decreased viabilities of human chronic myeloid leukemia cells under red light but not in dark, pointing the complex, itself, was not cytotoxic and singlet oxygen formation was required for the initiation of cell death mechanisms. Thus, **Ru-BP** can be effectively used as a photosensitizer in photodynamic therapy, which makes the novel **Ru-BP** a promising singlet oxygen generator for further biological applications.

View Article Online
DOI: 10.1039/C8NJ02944J

Introduction

Photodynamic therapy (PDT) has emerged as an innovative and non-invasive therapeutic modality for several types of cancers.[1-4] The primary components of PDT are a photosensitizer (PS), molecular oxygen and a light source. Following light excitation of the PS, an excited triplet state is formed which acts as an energy donor to molecular oxygen ($^3O_2$) to product reactive singlet oxygen ($^1O_2$).[5,6] The sensitized $^1O_2$ gives irreversible damage to tumour cells in the irradiated area. Photosensitizers are generally prepared from highly conjugated organic dyes and their transition metal complex, which can be monitored by various optical imaging techniques.[2,7-10] Compared to organic chromophores, transition metal complexes constitute another big family of medicinal agents.[11,12] Additionally, merging of organic chromophores with charge transfer complexes often leads to attractive properties such as unusual singlet and triplet state photophysics and related excited state dynamics.[13] Among these compounds, Ru (II)-based complexes are drawing great attention in the development of new photosensitizers due to their excellent biocompatibility and tuneable photophysical/chemical and excited-state properties.[7,12-16] Most of the Ru(II) PSs are based on polypyridyl ligands.[12,17,18] These complexes have long emission lifetimes from the triplet metal-to-ligand charge transfer state (MLCT) quenched by triplet (ground state) dioxygen and exhibit intriguing PDT effects *via* the type II process.[15,17,18] As in the most of the complex preparation, Ru(II)-based complexes also require a light-harvesting chromophore such as BODIPY (boron dipyrromethene), perylene or other cyclometaleted ligands.[7] The perylene unit, one of the most desirable molecules having large π-conjugation system, is a candidate to improve the optical properties of the complexes, to provide a red-shift of MLCT absorption band and an increased molar extinction coefficient of the metal complexes.[15,19,20] Furthermore, perylenes have high photochemical stability and fluorescence quantum yields

View Article Online
DOI: 10.1039/C8NJ02944J

in common aliphatic and aromatic solvents, resistivity towards oxidative degradation and decompositions.[19-22] Perylene chromophores are mainly used in the diimide form which receive widespread attention because of the molecular structure, rigid polycyclic aromatic core substituted from imide (peri) positions.[21] The disadvantage of perylene unit is its low solubility and aggregation that caused from its planar skeleton. In order to overcome the problem, perylene has been substituted from the bay positions in most of the studies.[22] Although many ruthenium(II) polypyridyl complexes and perylene dyes have been independently investigated as photosensitizers in the literature,[8,20] combination of these two units is very limited.[15] The success of the combination has encouraged us to focus on designing a novel complex bearing two perylenediimide (PDI) and a Ru(II) polypyridyl units at the same time in order to enhance photooxygenation ability. In the present study, a novel bis(perylenediimide) ruthenium(II) complex (**Ru-BP**) was prepared *via* reactions of two newly designed molecules, 5,6,12,13-tetrakis(4-(tert-butyl)phenoxy)-2-(2,6-diisopropylphenyl)-9-(4-hydroxyphenyl) anthra[2,1,9-def:6,5,10-d'e'f']diisoquinoline-1,3,8,10(2H,9H)-tetraone (**P6**) and 4,7-dichlorophenanthroline ruthenium(II) complex (**7**) (Figure 1). Generally, ruthenium complexes coordinated by phenanthroline derivatives are substituted from 5- or 5,6- positions with several chromophores and a few perylene substituted derivatives of those are also connected from 5-position of phenanthroline moiety.[23] The present study can be accepted as the first example of modification of two perylenediimide unit attached from 4,7-positions of phenanthroline metal complex.[15,19,20] The photophysical and singlet oxygen generation properties of the novel **Ru-BP** was investigated *via* absorption and fluorescence spectroscopies. In addition, the photodynamic therapy efficacy of **Ru-BP** complex was assessed in human chronic myeloid leukemia cells *in vitro*. Overall, this study presents novel and fully characterized **Ru-BP** complex with fundamental photodynamic therapy efficiency.

View Article Online
DOI: 10.1039/C8NJ02944J

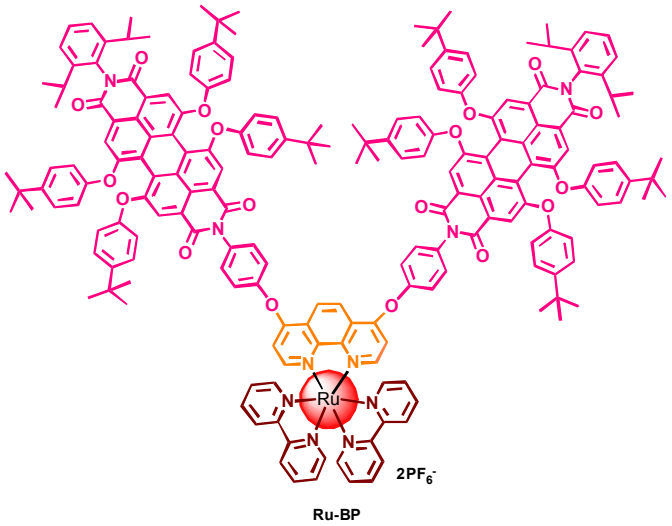

Ru-BP

Fig. 1 Structure of new bis(perylenediimide) ruthenium(II) complex (**Ru-BP**).

Results and discussion

Syntheses and characterizations

The synthesis of **Ru-BP** is depicted in Scheme 1. First, the synthesis of new ruthenium complex (**7**) was carried out *via* reaction between 4,7-dichloro-1,10-phenanthroline (**5**)[24] and ruthenium(II) bis(bipyridinyl) complex (**6**)[25] in ethanol/H_2O reaction medium. Without advanced purification steps, the crude material was used for further reaction. Next, synthesis of perylene diimide **P6** was conducted in five steps (Scheme 1). After bromination of **P1** to obtain **P2**,[26] preparation of diimide **P3**[27] was employed using 2,6-diisopropylaniline as aromatic amine. Then, 4-*tert*-butylphenol was used to substitute bay positions of **P3** in order to prepare **P4**.[28] After synthesizing monoimide monoanhydride **P5**[29] in KOH basic medium, desired perylenediimide **P6** was prepared using 4-aminophenol as a reagent. Single molecular ion peak in the mass spectrum supports the purity of the compound. (Fig. S3). In the FT-IR spectrum of **P6** the disappearance of anhydride band at 1770 cm^{-1} confirms the assigned structure. Also, C=O bands of imide group was observed at 1672 and 1705 cm^{-1} (Fig.

View Article Online
DOI: 10.1039/C8NJ02944J

S4). Additionally, the ^{1}H-NMR and ^{13}C-NMR spectra are consistent with the molecular structure of **P6** (Fig. S5,S6).

View Article Online
DOI: 10.1039/C8NJ02944J

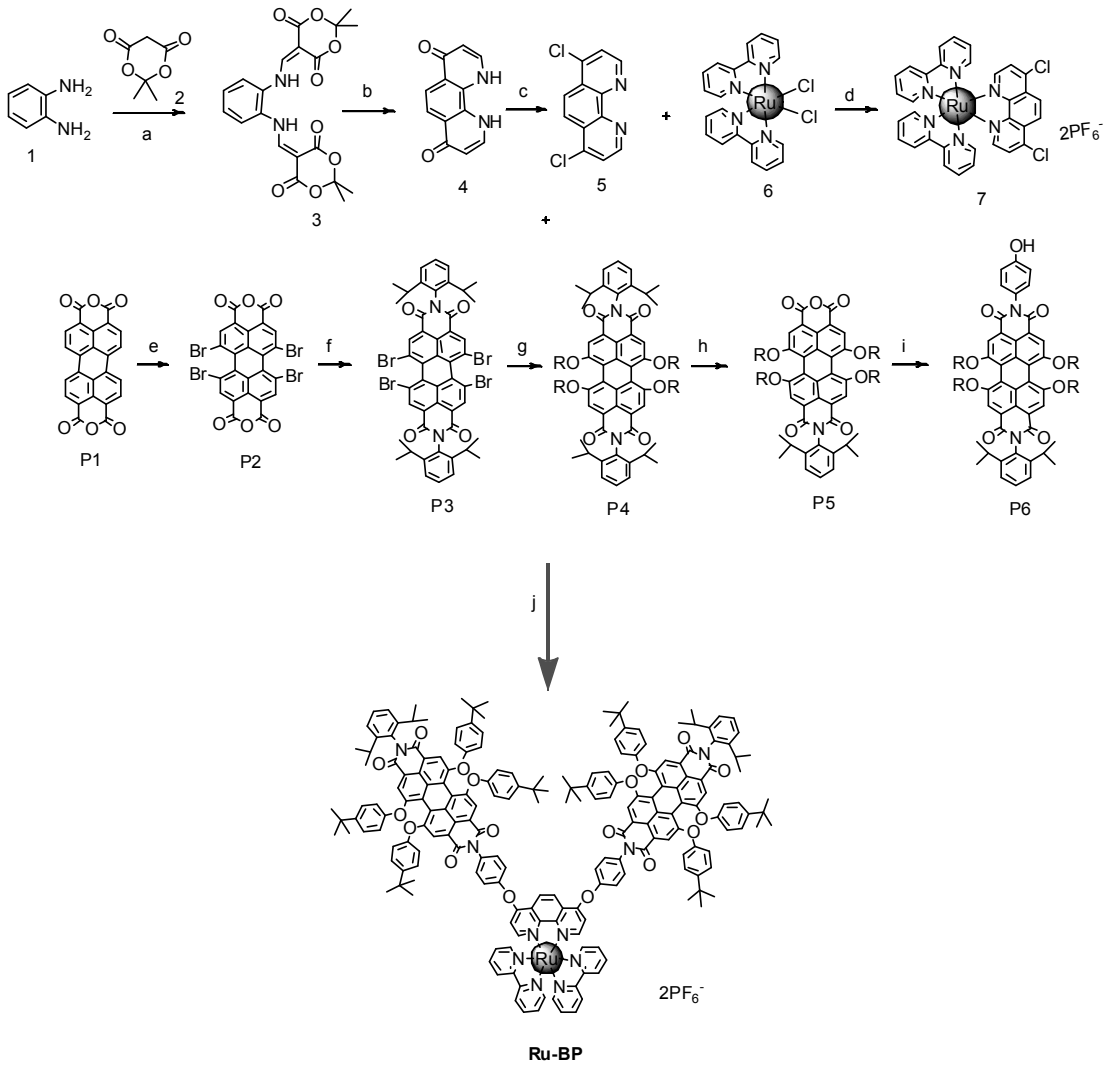

Scheme 1 Synthesis of **Ru-BP**. Reagents and conditions: (a) Meldrum's acid (2.3 equiv.) ,$CH(OMe)_3$, reflux, 3h (b) diphenyl ether, reflux, 30 min (c) $POCl_3$, reflux, 2h [23] (d) **6**,[24] EtOH/ H_2O, reflux, 16 h; (e) Br_2, H_2SO_4, rt→120 ˚C, 96 h[25] (f) 2,6-diisopropylaniline (2 equiv.), propionic acid, reflux, 24 h[26] (g) 4-tert butylphenol (8 equiv.), K_2CO_3, NMP, reflux, 24 h[27] (h) KOH, t-BuOH, reflux, 30 min[28] (i) 4-amino phenol (1 equiv.) , propionic acid, reflux, 24 h (j), rt, 72h.

View Article Online
DOI: 10.1039/C8NJ02944J

Nucleophilic substitution reaction of **P6** and **7** leads to **Ru-BP** as a dark purple solid (Scheme 1). The mass spectrum of **Ru-BP** confirms the molecular structure. The molecular ion peak is observed at as $[M\text{-}2PF_6]^+$. Also, the peak observed at *m/z* 3204 belongs to $[M\text{-}PF_6]^+$ (Fig. S7). In the FT-IR spectrum of **Ru-BP** the expected imide C=O bands appear at 1671 and 1705 cm^{-1} similar as **P6** and the absence of hydroxyl peak at around 3400 cm^{-1} supports the structure. The peak around 830 cm^{-1} belongs to the PF_6^- counter ion[30] of the structure (Fig. S8). The ^{1}H-NMR (Fig. S9) and ^{13}C-NMR spectra (Fig. S10) of **Ru-BP** are consistent with the structure of **Ru-BP**. Integration ratios and chemical shift values were assigned in Fig. S9 and Fig. S10. Aromatic protons of the structure appear between 8.7-6.8 ppm. Distinctly, compared to the ^{1}H-NMR of **P6**, specific phenanthroline protons of the complex **Ru-BP** arise at 8.6 ppm. Tertiary protons of diisopropyl amino group were observed at 2.7 ppm. Methyl protons of phenoxy cores give a singlet at 1.26 ppm while diisopropyl groups' appear at 1.11 ppm as doublet.

Also, **Ru-BP** is highly soluble in common organic solvents such as dichloromethane, chloroform, tetrahydrofuran (THF) and dimethylsuphoxide (DMSO) and it is stable below 200 °C according to the thermogravimetric analysis (TGA) (Fig S11).

Photophysical properties of Ru-BP in comparison with P6

Spectral characterization of **Ru-BP** was carried out recording absorption, excitation and emission spectra in dimethylsulphoxide (DMSO) at room temperature. To study the effect of the Ru(II) phenanthroline chromophore, same spectroscopic studies were also carried for newly synthesized **P6**. The UV-vis absorption spectra of **P6** and **Ru-BP** are shown in Figure 2. Absorption maxima together with molar extinction coefficients are depicted in Table 1. The spectra of **P6** and **Ru-BP** show a similar profile bearing four maxima observed approximately

View Article Online
DOI: 10.1039/C8NJ02944J

at 260, 285, 450 and 580 nm. The overlap of characteristic π- π* transition of PDI and MLCT transitions appeared between 440 and 590 nm.[31] The increase in the absorption intensity at 260-290 nm region indicates the existence of Ru(II) bipyridyl moiety in the main structure. Additionally, molar extinction coefficient of **Ru-BP** is higher than the **P6**'s as indicated in Table 1. The ground state absorption spectra of **P6** and **Ru-BP** were also recorded at different concentrations (Fig. S12 and S13). The emission properties of **P6** and **Ru-BP** were studied in DMSO at room temperature (Table 1). The patterns of emission behavior of **P6** and **Ru-BP** were similar, and their emission maxima were 614 and 615 nm. For both compounds, the excitation spectra were similar to the corresponding absorption spectra and the both excitation and absorption spectra were mirror image of their own fluorescence emission spectra. The Stoke's shift was found to be 34 nm for **P6** and 33 nm for **Ru-BP**. The fluoroscence lifetimes (τ_F) of **P6** and **Ru-BP** was measured using the time correlated single photon counting (TCSPC) technique in DMSO. Obtained lifetime spectra are shown in Fig S16. The lifetimes were found to be 2.09 ns for **P6** and 1.04, 5.65 for **Ru-BP**. The absorption and emission profiles of **Ru-BP** is suitable for in *vivo* photooxidation and deeper penetration in tissue.[1,3]

View Article Online
DOI: 10.1039/C8NJ02944J

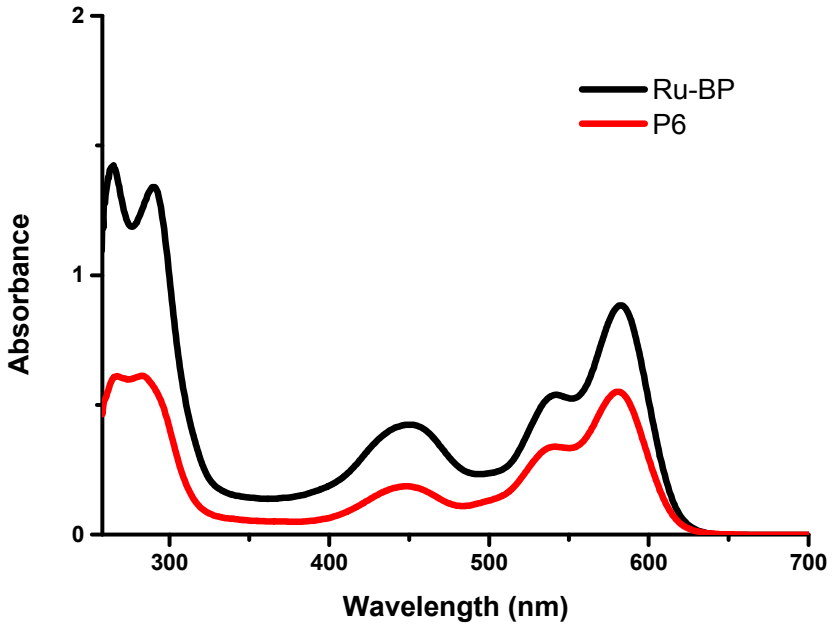

Fig. 2 UV-vis absorption spectra of **P6** and **Ru-BP** in DMSO.

Table 1 Photophysical and photochemical properties of **P6** and **Ru-BP** [a].

Compound	λ_{ab}, nm (Log ε[b])	λ_{em}, nm	τ_F (ns)[c]	[d]ϕ_Δ
P6	267 (4.74), 283 (4.77), 449 (4.33), 580 (4.78)	614	2.09 (CHISQ=0.9899979)	0.01
Ru-BP	264 (11.85), 290 (11.80), 451 (4.62), 582 (4.94)	615	1.04 (23.6 %) 5.65 (76.4 %) (CHISQ = 0.9366626)	0.30

[a] dimethylsulphoxide [b] Molar extinction coefficients [c] Lifetime [d]Singlet Oxygen Quantum Yield

View Article Online
DOI: 10.1039/C8NJ02944J

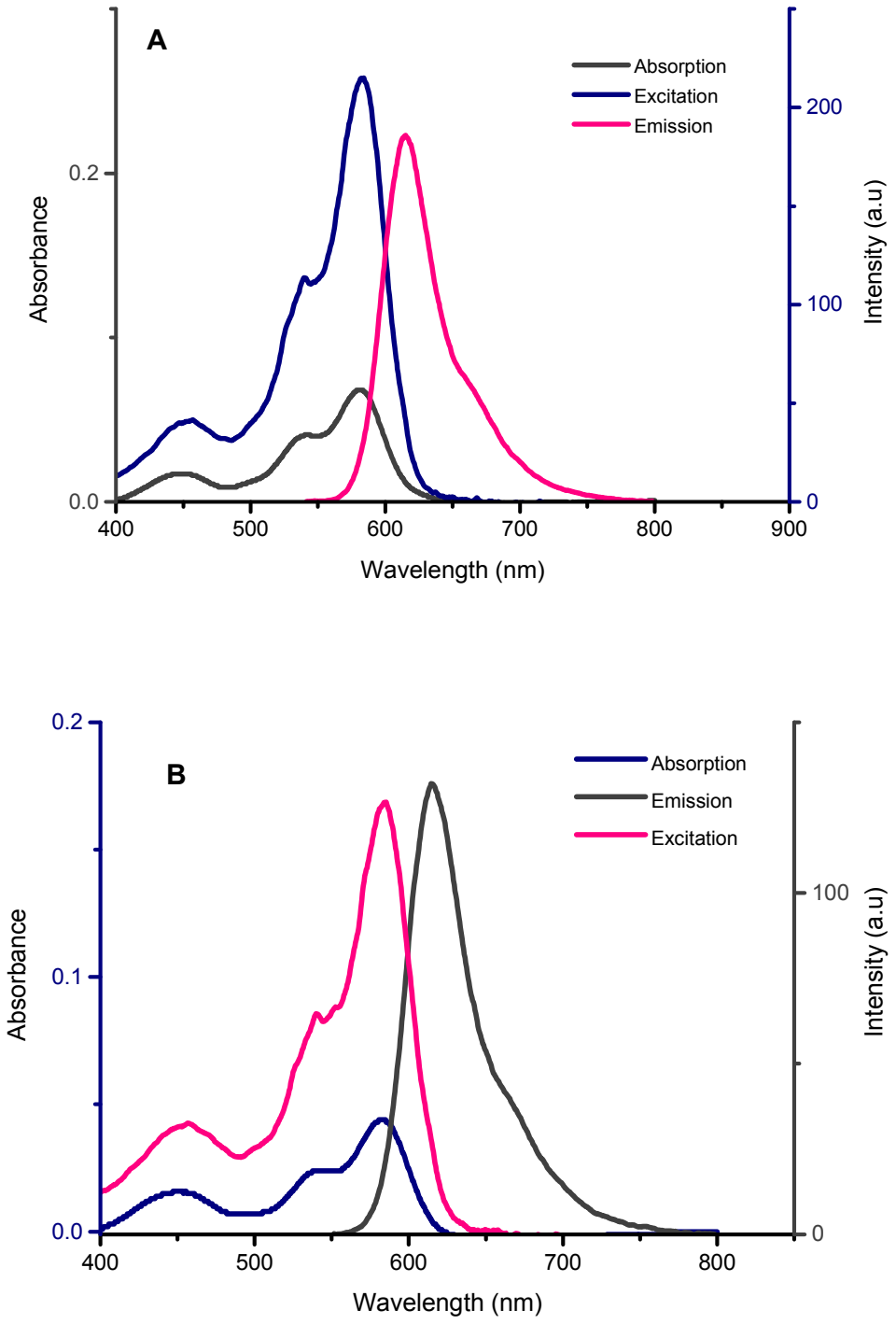

Fig. 3 UV-vis, fluorescence emission and excitation spectra of **P6** (0.5 μM) (**A**) and **Ru-BP** (2.0 μM) (**B**)

View Article Online
DOI: 10.1039/C8NJ02944J

Photosensitizing property of Ru-BP

The mechanism of type II PDT is based on energy transfer from triplet state of the photosensitizers to molecular oxygen for generating singlet oxygen ($^1O_2$) which can instantaneously damage biomolecules to initiate cell death.[6] Investigating the generation of $^1O_2$ is highly significant to pre-study PDT application at the molecular level. In this work, singlet oxygen generation capacity of novel bis(perylenediimide) ruthenium (II) complex (**Ru-BP**) was performed using diphenylisobenzofuran (DBPF), selective singlet oxygen trap molecule, in DMSO. A solution of the **Ru-BP** (2.0 μM) and DPBF (35.0 μM) was kept for 20 min in the dark to eliminate any inputs to the absorbance signal of DPBF from obscure dark reactions. Absorption band of DPBF at 414 nm did not show any change proved the lack of dark reactions. The mixture of the **Ru-BP** and DPBF was irradiated with red light (λ= 632 nm, 2.5 mW /cm^2) for a time interval 0 to 24.0 min. Photo-induced production of singlet oxygen from **Ru-BP** was monitored gradual decrease in the absorption intensity of DPBF (Fig. 4). The data for **Ru-BP** was plotted as the change in absorption of the trap molecule at 414 nm versus irradiation time (Fig.4). Also, singlet oxygen measurements of the **P6** (2.0 μM) and methylene blue (2.0 μM) as the reference molecule were performed under the same experimental conditions (Fig. S14, S15). Singlet oxygen quantum yields (Φ_Δ) of free ligand **P6** and **Ru-BP** were calculated according to the literature.[32] The singlet oxygen quantum yield of **Ru-BP**(Φ_Δ=0.30) is thirty times higher than the free ligand **P6** (Φ_Δ=0.01) (Fig. S15). The attractive increase of the Φ_Δ would be explained by heavy atom effect that has been widely known as the most popular way to facilitate the intersystem crossing (ISC) of the chromophore.[7] In the present work, singlet oxygen generation showed good efficiency when compared with reported ruthenium(II) or ruthenium perylene photosensitisers.[14,15] The

View Article Online
DOI: 10.1039/C8NJ02944J

photostability upon repetitive excitation and is desirable in PDT application.[1,7] The solution of **Ru-BP** without DPBF were triggered with light for 20 min and no change was observed in the absorbance intensity of compound in the red region of the spectrum (Fig. S17). It is obvious that this complex was not degraded under the condition of singlet oxygen measurements.

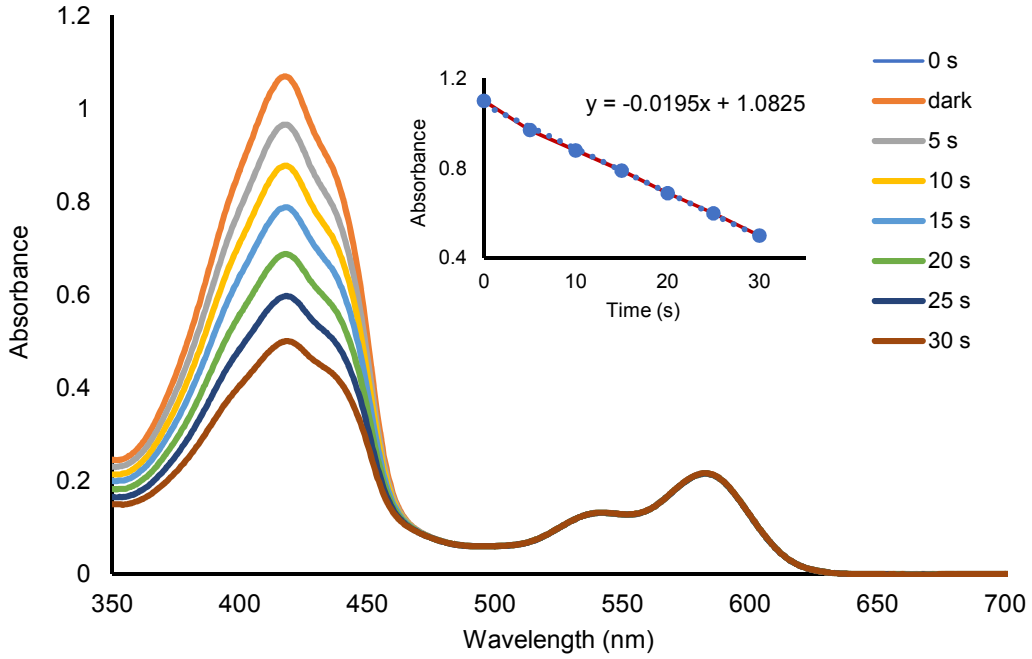

Fig. 4 Decrease in absorbance spectrum of DPBF (35.0 µM) in the presence of **Ru-BP** (2.0 µM) in DMSO and absorbance decrease of DPBF at 414 nm with time in DMSO in the presence of **Ru-BP**.

In vitro photodynamic therapy

In the present study, we also aimed to study the photodynamic therapy efficacy of **Ru-BP** after chemical characterization. Ruthenium complexes and their *in vitro* and/or *in vivo* efficacy have been widely used in photodynamic therapy studies for effective treatment of cancer.[16,17,33] To check the efficacy of **Ru-BP** in terms of photodynamic therapy, we used

View Article Online
DOI: 10.1039/C8NJ02944J

human chronic myeloid leukemia cell line, K562. We treated cells with increasing concentrations of **Ru-BP** and incubated the cells either under red light (λ= 632 nm, 2.5 mW /cm^2) or in dark for 5 h. Next, we determined the cell viabilities by MTT assay. According to results (Fig. 5), **Ru-BP** complex significantly decreased cell viabilities if only the cells were incubated under red light but not in dark. The ability of **Ru-BP** in the production of singlet oxygen by red light source was demonstrated in Fig. 4 Singlet oxygen, whether intracellular or extracellular, is able to trigger apoptosis, a type of well-regulated cell death mechanism.[34] Fig. 5 proves that **Ru-BP**, itself, was not enough to trigger cell death in dark but a red light source was needed to produce singlet oxygen and cause death of cancer cells. However, this data is not enough to determine the cell death type, whether apoptotic or not, which requires further molecular studies. Also, **P6**, itself, at maximum concentration of **Ru-BP** tested was not successful to induce cell death in dark or under red light, confirming the chemical characterization studies of **P6**, which was shown to produce limited singlet oxygen compared to **Ru-BP**, on cells. The inhibitory concentration 50 (IC_{50}) value for **Ru-BP** was calculated as below 5.0 μM while could not be calculated when they were treated in dark, pointing the success of light-excited **Ru-BP** in the initiating cell death.

View Article Online
DOI: 10.1039/C8NJ02944J

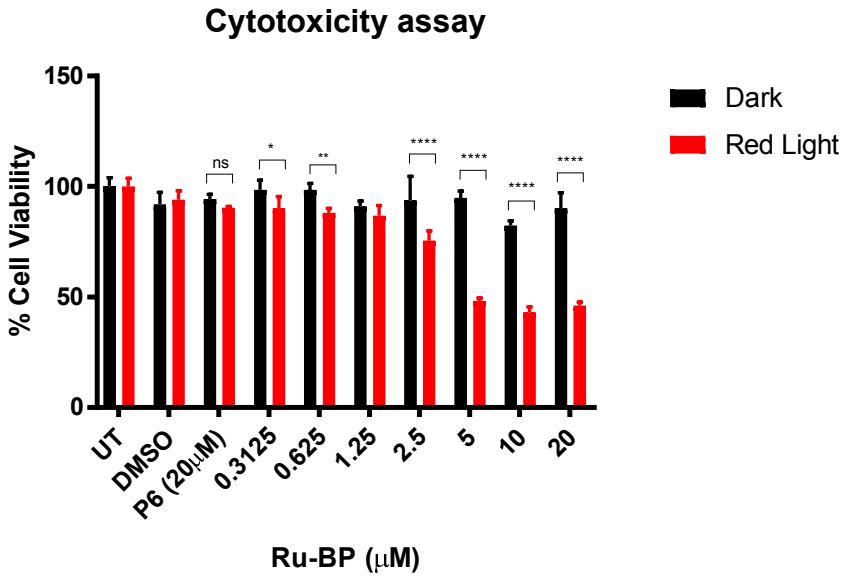

Fig. 5 *In vitro* photodynamic therapy efficacy. *p<0.05; **p<0.01; ****p<0.0001.

To further show the ability of **Ru-BP** in the induction of cell death in the presence of red light, we used Trypan Blue staining. It is a dye widely used in cell culture and cannot penetrate into living cells while it internalizes into and stains the nonviable cells blue.[35] In this study, we treated cells with Trypan Blue in absence or presence of **Ru-BP** and under light or in dark. According to the results, the blue colour that is a sign of nonviable cells was only available for **Ru-BP**-treated cells under red irradiation. Ruthenium complexes have been widely used in photodynamic therapy studies. However, some problems, such as, high IC_{50} value,[36] increased toxicity of photosensitizer without irradiation,[37] long incubation time of photosensitizer[38] and irradiation under lower wavelengths preventing deep tissue penetration[39] have been faced during these studies. The present study is critical in terms of overcoming listed drawbacks of ruthenium-based photodynamic therapy studies owing to low cytotoxicity of **Ru-BP** in dark (Fig. 5), relatively low IC_{50} value (<5 μM), short incubation

View Article Online
DOI: 10.1039/C8NJ02944J

time to induce cell death (5 h) and irradiation with red light which increases the tissue penetration depth. Still, further *in vivo* studies are needed to conclude the effectiveness of **Ru-BP** in clinics.

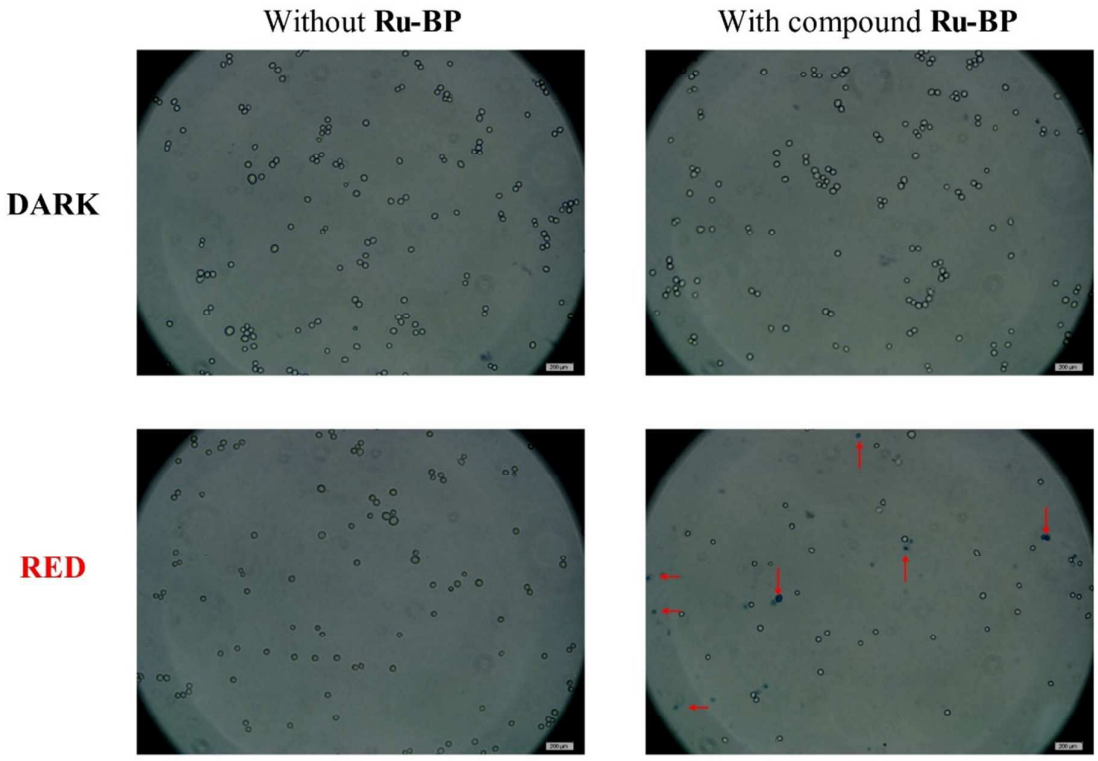

Fig. 6 Trypan Blue staining of **Ru-BP**-treated or –untreated cells in dark or under red light. Red arrows point the blue-coloured cells. Scale: 200 µm.

Experimental Section

General methods

Perylene-3,4,9,12-tetracarboylic dianydride, 1,10-phenanthroline, tetrabutylammonium hexafluorophosphate and $RuCl_3.H_2O$ was obtained from Sigma-Aldrich. All reagents and solvents were of reagent-grade quality, obtained from commercial

View Article Online
DOI: 10.1039/C8NJ02944J

suppliers. Infrared spectra were recorded between 4000 and 650 cm^{-1} by using a Perkin Elmer Spectrum100 FT-IR spectrometer with an attenuated total reflection (ATR) accessory featuring a zinc selenide (ZnSe) crystal. The mass spectra were recorded on a MALDI (Matrix Assisted Laser Desorption Ionization) BRUKER Microflex LT using 1,8,9-anthrasenetriol (dithranol) as a matrix. The NMR spectra were recorded on a Varian INOVA 500 MHz spectrometer. Electronic absorption spectra were recorded with a Shimadzu 2101 UV spectrophotometer and the fluorescence excitation and emission spectra were recorded on a Varian Eclipse spectrofluorometer using 1 cm pathlength cuvettes at room temperature. Fluorescence lifetimes were measured by a time correlated single photon counting (TCSPC) method using FLUOROLOG-3 spectrofluorometer (Horiba JobinYvon, Edison, NJ) equipped with a NanoLED and a standard air cooled R928 PMT detector. Photo-irradiations were done using a red LED (λ= 632 nm, 2.5 mW /cm^2) and samples were irradiated with the light source from a 10.0 cm distance.

Singlet Oxygen Measurements

Singlet oxygen quantum yields (Φ_Δ) were calculated according to the literature.[32] The relative quantum yields were calculated with reference to Methylene Blue (MB) in DMSO as 0.52.[40] Air saturated DMSO was obtained by bubbling air for 30 minutes. The absorbance of DPBF was adjusted around 1.0-1.1 in air saturated DMSO. Then, the sample was added to cuvette and sample's absorbance was adjusted around 0.1-0.2. After, taking some measurements in dark, we exposed the cuvette to red LED at the peak absorption wavelength for 5 s. Absorbance was measured for several times after each irradiation. Then, slope of absorbance maxima of DPBF at 414 nm versus time graph for each sample was calculated. Singlet oxygen quantum yield was calculated according to the equation:

View Article Online
DOI: 10.1039/C8NJ02944J

Φ_Δ (samp) = Φ_Δ (ref) × [m (samp)/m(ref)]×[F(ref)/F(samp)]

"m" is the slope of difference in change in absorbance of DPBF (414 nm) with the irradiation time, "F" is the absorption correction factor, which is given by F = 1 – 10^{-OD} (OD at the irradiation wavelength).

Synthesis of 7. Compound 5 and 6 were prepared according to the reported procedures.[24,25] A mixture of **5** (52 mg, 0.21 mmol) and **6** (0.1 g, 0.21 mmol) was refluxed in Ethanol/H_2O (15 mL/7 mL) for 16 h.(Scheme 1) After cooling, NH_4PF_6 (0.6 g, 3.68 mmol) was added to the mixture. Resulting orange solid was washed with water and diethyl ether. ATR-IR ν_{max} (cm^{-1}): 3325, 3123, 1606, 1560, 1469, 1446, 1412, 1395, 1336, 1316, 1245, 1219, 1085, 821, 760, 730 cm^{-1}. MS: MALDI-TOF (dithranol): m/z: 662 $[M\text{-}2PF_6]^+$, 629 $[M\text{-}2PF_6\text{-}Cl]^+$ (Fig. S1, S2).

Synthesis of P6. From **P1** to **P5** literature procedure[26-29] was employed. A mixture of 4-aminophenol (0.01 g, 0.1 mmol) and (55.0 mg, 0.05 mmol) of **P5** was refluxed under Ar atmosphere in 5 mL propionic acid. After 24 h, the mixture was extracted with H_2O/CH_2Cl_2. Preparative thin layer chromatography on silica gel (CH_2Cl_2) yielded 25 mg (42% yield) of **P6**. ^{1}H-NMR ($CDCl_3$) δ 8.28 (s, 2H), 8.23 (s, 2H), 7.41(t, *J* = 8.0 Hz, 2H), 7.25-7.21 (m, 10H), 7.08 (d, *J* = 8.5 Hz, 2H), 6.88 (t, *J* = 10 Hz, 5H), 6.83 (d, *J* = 8.5 Hz, 4H), 2.70 (septet, *J* = 7.0 Hz, 2H), 1.26 (d, *J* = 4.0 Hz, 36 H), 1.11 (d, *J* = 7.0 Hz, 12H). ^{13}C-NMR ($CDCl_3$): 164.051, 163.578, 156.241, 156.211, 155.921, 153.076, 152.958, 147.638, 147.558, 145.832, 133.392, 130.9, 129.846, 129.609, 127.969, 126.894, 124.093, 122.933, 122.75, 121.077, 120.878, 120.496, 120.362, 120.031, 119.545, 119.411, 116.415, 34.58, 31.638, 29.922, 29.29, 24.229. ATR-IR ν_{max} (cm^{-1}): 3406, 3063, 3039, 2962, 2930, 2869, 1705, 1672, 1585, 1504, 1464, 1447, 1407, 1363, 1341, 1315, 1283, 1220, 1173, 882, 832 cm^{-1}. UV (DMSO): λ_{max} = 267, 283, 449, 580 nm. MS: MALDI-TOF (dithranol): m/z: 1235 $[M^+]$, 1257 [M+ 2H] (Fig. S3-S6).

View Article Online
DOI: 10.1039/C8NJ02944J

Synthesis of Ru-BP. A mixture of **7** (0.02 g, 0.03 mmol), **P6** (75.0 mg, 0.06 mmol) and K_2CO_3 (8.2 mg, 0.06mmol) was stirred at room temperature under Ar in DMF (Scheme 1). After 72 h, the mixture was extracted with H_2O/CH_2Cl_2. Chromatography on silica gel (CH_2Cl_2 → CH_2Cl_2 /EtOH (50/1) yielded 60 mg (60% yield) of **Ru-BP**. ^{1}H-NMR ($CDCl_3$) δ 8.61 (s, 2H), 8.30-8.27 (m, 8H), 8.24 (s, 4H), 7.93-7.91 (m, 4H), 7.86-7.83 (m, 4H), 7.59 (d, *J* = 6.0 Hz, 2H), 7.47-7.38 (m, 14 H), 7.25-7.20 (m, 21H), 6.99 (d, *J* = 6.0 Hz, 2H), 6.86-6.82 (m, 15 H), 2.7 (septet, *J* = 6.5 Hz, 4H), 1.26 (s, 72 H), 1.11 (d, *J* = 6.5 Hz, 24H). ^{13}C-NMR ($CDCl_3$) 181.369, 180.874, 163.607, 163.557, 163.491, 162.62, 157.399, 156.399, 156.336, 156.122, 153.066, 152.878, 152.672, 152.572, 148.184, 147.585, 145.817, 137.826, 137.564, 137.477, 133.918, 133.413, 133.375, 131.507, 130.883, 129.7, 129.615, 129.194, 128.773, 128.083, 127.104, 126.88, 126.704, 126.649, 124.094, 123.87, 123.682, 123.59, 123.422, 123.004, 122.376, 122.268, 122.164, 122.094, 121.375, 120.725, 120.633, 120.545, 120.336, 120.3, 120.05, 119.628, 119.489, 119.458, 119.327, 119.276, 116.872, 110.364, 34.715, 34.578, 34.436, 33.395, 32.142, 31.835, 31.779, 31.652, 31.5, 29.917, 29.665, 29.578, 29.496, 29.461, 29.386, 29.298, 24.972, 24.239, 22.91, 14.338. ATR-IR v_{max} (cm^{-1}): 3067, 2962, 2906, 2869, 1705, 1671, 1585, 1501, 1466, 1405, 1363, 1339, 1281, 1206, 1173, 1110, 1014, 834, 761, 729 cm^{-1}. UV (DMSO): λ_{max} = 264, 290, 448, 551, 582 nm. MS: MALDI-TOF (dithranol): m/z: 3060 [M-2PF_6], 3204 [M-PF_6] (Fig. S7-S10).

Cell lines and cell culture

In this study, human chronic myeloid leukemia, K562 cell line was used for photodynamic therapy studies. Cells were maintained in RPMI 1640 medium (Biochrom AG, Germany) in the presence of 10% FBS (v/v; Biochrom AG, Germany) and 1% gentamycin (v/v; Biological Industries, Israel) at 37^{o}C and 5% CO_2.

View Article Online
DOI: 10.1039/C8NJ02944J

Cell viability assay

Cell viabilities were analyzed by 3-(4,5-dimethylthiazol-2-yl)-2,5 diphenyltetrazolium bromide (MTT) assay. $30x10^3$ cells were seeded into two different 96-well plates and incubated for 24h. Next, cells were treated DMSO to check the solvent effect and increasing concentration of Ru-BP (0.3125-20 µM). One of the plates was incubated in dark while the other was incubated under red LED for 5 hours. Then, 10 µl of MTT solution (5mg/ml) was added onto cells and incubated for 4h. Finally, cells were disrupted with SDS-HCl solution (1g SDS in 0.01M HCl in 10ml final volume) overnight and the microplates were read by microplate spectrophotometer (Multiskan GO, Thermo Fisher Scientific, USA) at a wavelength of 570 nm. Optical densities were converted to % viability by using untreated cells as 100% and all the treatments were correlated to untreated group. Data were analyzed by GraphPad Prism 7.0 software (GraphPadInc, USA). The results were considered significant at the level of 0.05.

Trypan Blue staining

To further demonstrate the cell death, $480x10^3$ cells were treated into two different 6-well plates. One of the well of each plates was treated with 20.0 µM of **Ru-BP** and one of them was treated with DMSO as control. One of the plates was incubated in dark while the other was treated red light for 5 h. Next, cells were incubated with Trypan Blue (10%) for 5 min and washed by PBS twice. Next, cells were imaged under a light microscope.

Statistical analyses

All biological experiments were conducted triplicate as three independent experiments. Data were analysed by Two-way ANOVA and was evaluated as significant when $p<0.05$.

View Article Online
DOI: 10.1039/C8NJ02944J

CONCLUSIONS

In this work, we demonstrated design, synthesis and photooxygenation of a novel ruthenium phenanthroline bis(perylenediimide) complex (**Ru-BP**). The newly synthesized **Ru-BP** and its starting compound, **P6** were fully characterized by FT-IR, MALDI-TOF, ^{1}H and ^{13}C-NMR, UV-vis spectroscopy analyses. The novel **Ru-BP** possesses two PDI core in a ruthenium(II) complex that is the first example of bis(perylenediimide) substituted phenanthroline metal complex. The photophysical and photochemical properties of the novel **Ru-BP** was investigated *via* absorption and fluorescence spectroscopies in comparison with **P6**. **Ru-BP** exhibited favourable photophysical properties in the red region with good molar extinction coefficient. It is obvious from the singlet oxygen quantum yields that ruthenium complex form of **P6** leads to a respectable photosensitizer ability. Moreover, novel **Ru-BP** complex displayed significant photodynamic therapy efficacy *in vitro*. **Ru-BP** efficiently decreased the survival of human chronic myeloid cells, K562 under red light but not in dark. This result also confirms the production of singlet oxygen by **Ru-BP** *in vitro* by which cell death mechanisms were activated. The novel **Ru-BP** complex is also a strong candidate for *in vivo* photodynamic therapy studies due to its low toxicity in dark, low IC_{50} value, short incubation time and possible longer tissue penetration depth. Overall, the results described herein clearly indicate that the novel complex **Ru-BP** is a potential singlet oxygen generator for PDT processes. Thus, our *in vivo* animal model studies are under progress.

ACKNOWLEDGEMENTS

This work was financially supported by the Gebze Technical University Research Project Foundation, BAP-2017 -A102-15.

REFERENCES

View Article Online
DOI: 10.1039/C8NJ02944J

1 R. Bonnett, *Chemical Aspects of Photodynamic therapy*, Gordon & Breach, London, UK, 2000.

2 J. P. Celli, B. Q. Spring, I. Rizvi, C. L. Evans, K. S. Samkoe, S. Verma, B. W. Pogue, T. Hasan, *Chem. Rev.*, 2010, **110**, 2795–2838.

3 M. Ethirajan, Y. Chen, P. Joshi, R. K Pandey, *Chem. Soc. Rev.,* 2011, **40**, 340–362.

4 S. H. L. Higgins, K. J. Brewer, *Angew. Chem*., *Int. Ed.*, 2012, **51**, 11420–11422.

5 S. G. Awuahaband, Y. You, *RSC Adv.*, 2012, **2**, 11169-11183.

6 J. F. Lovell, T. W. B. Liu, J. Chen, G. Zheng, *Chem. Rev.*, 2010, **110**, 2839-57.

7 J. Zhao, W. Wu, J. Sun, S. Guo, *Chem. Soc. Rev.*, 2013, **42**, 5323-5351.

8 F. Yukruk, A. L. Dogan, H. Canpinar, D. Guc, E. U. Akkaya, *Org. Lett.*, 2005, **7**, 2885-2887.

9 A. Wang, W. Jin, E. Chen, J. Zhou, L. Zhou, S. Wei, *Dalton Trans.*, 2016, **45**, 3853-3862.

10. A. Kamkaew, S. H. Lim, H. B. Lee, L. V. Kiew, L. Y. Chungc, K. Burgess, *Chem. Soc. Rev.*, 2013, **42**, 77-88.

11. C. G. Hartinger, P. J. Dyson, *Chem. Soc. Rev.*, 2009, **38**, 391–401.

12 Q. X. Zhou, W. H. Lei, J. R. Chen, C. Li, Y. J. Hou, X. S. Wang, B. W. Zhang, *Chem. Eur. J.*, 2010, **16**, 3157 – 3165.

13 F. N Castellano, *Acc. Chem. Res*., 2015, **48**, 828-839.

14 Z. Lv., H. Wei, Q. Li, . Su, S. Liu, K. Y. Zang, W. Lv, Q. Zao, X. Li, W. Huang, *Chem. Sci.*, 2018, **9**, 502–512.

15 P. J. S. Maiaa, I. Aguiarb, M. S. Vellosoc, D. Zhangd, E. R. Santosb, J. R. Oliveirac, J. C. Junqueirac, M. Selked, R. M. Carlosb, *J. Photochem. Photobiol., A*, 2018, **353**, 536–545.

16. P. Kaspler, S. Lazic, S. Forward, Y. Arenas, A. Mandela, L. Lilge, *Photochem. Photobiol. Sci.*, 2016, **15**, 481–495.

17 H. Huang, B. Yu, P. Zhang, J. Huang, Y. Chen, G. Gasser, L. Ji, H. Chao, *Angew. Chem., Int. Ed.*, 2015, **54**, 14049.

18 J. Liu, Y. Chen, G. Li, P. Zhang, C. Jin, L. Zeng, L. Ji, H. Chao, *Biomaterials*, 2015, **56**, 140.

19 K. Kodama, A. Kobayashi, T. Hirose, *Tetrahedron Lett.,* 2013, **54**, 5514–5517.

View Article Online
DOI: 10.1039/C8NJ02944J

20 E. R. Santos, J. Pina, T. Venâncio, C. Serpa, J. M. G. Martinho, R. M. Carlos, *J. Phys. Chem. C*, 2016, **120**, 22831−22843.

21 F. Würthner, C. R. Saha-Möller, B. Fimmel, S. Ogi, P. Leowanawat, D. Schmidt, *Chem. Rev.*, 2016, **116**, 962−1052.

22. F. Würthner, C. Thalacker, A. Sautter, *Adv. Mater.*, 1999, **11**, 754-758.

23 R. K. Dubey, M. Niemi, K. Kaunisto, K. Stranius, A. Efimov, N. V. Tkachenko, H. Lemmetyinen, *Inorg. Chem.*, 2013, **52**, 9761−9773.
24 F. Molock, D. W. Boykin, *J. Heterocycl. Chem.*, 1983, **20**, 681-686.

25 Y. Nakabayashi, Y. Watanabe, T. Nakao, O. Yamauchi, *Inorg. Chim. Acta*, 2004, **357**, 2553.

26 W. Qiu., S. Chen, X. Sun, Y. Liu, D. Zhu, *Org. Lett.*, 2006, **8**, 867-870.
27 Z. B. Hill, D. B. Rodovsky, J. M. Legera, G. P. Bartholomew, *Chem. Comm.*, 2008, 6594-96.

28 H. Quante, P. Schlichting, U. Rohr, Y. Geerts, K. Müllen, *Macromol. Chem. Phys.,* 1996, **197**, 4029-44.

29 L. D. Wescott, D. L. Mattern, *J. Org. Chem.*, 2003, **68**, 10058-66.

30 J. G. Wang, Y. L. Shang, *Mater. Res. Innovations*, 2013, **17**, 58-61.

31 F. Würthner, *Chem. Commun*., 2004, 1564–1579.

32 N. Adarsh, M. Shanmugasundaram, R. R. Avirah, D. Ramaiah, *Chem. Eur. J.*, 2012, **18**, 12655-62.

33 L. Zheng, S. Kuang, G. Li, C. Jin, L. Ji, H. Chao, *Chem. Commun.*, 2017, **53**, 1977-1980.

34 M. Reithmuller, N. Burger, G. Bauer, *Redox Biology*, 2015, **6**, 157-168.

35 N. Barekzi, M. Laroussi, G. Konesky, S. Roman, *Plasma Process Polym.,* 2016, **13**, 1189-1194.

36 W. Li, Q. Xie, L. Lai, Z. Mo, X. Peng, E. Leng, D. Zhang, H. Sun, Y. Li, W. Mei, S. Gao, *Photodiagn. Photodyn.*, 2017, **18**, 83-94.

37 K. Qiu, J. Wang, C. Song, L. Wang, H. Zhu, H. Huang, J. Huang, H. Wang, L. Ji, H. Chao, *ACS Appl. Mater Interfaces*, 2017, **9**, 18482-18492.

38 H. Huang, P. Zhang, B. Yu, C. Jin, L. Ji, H. Chao, *Dalton Trans.*, 2015, **44**, 17335-17345.

39 H. Yu, J. Liu, Z. Hao, J. He, M. Sun, S. Hu, L. Y, H. Chao, *Dyes Pigments,* 2017, **136**, 416-426.

40 N. Adarsh, R. R. Avirah, D. Ramaiah, *Org. Lett.* 2010, **12**, 5720-5723.

View Article Online
DOI: 10.1039/C8NJ02944J

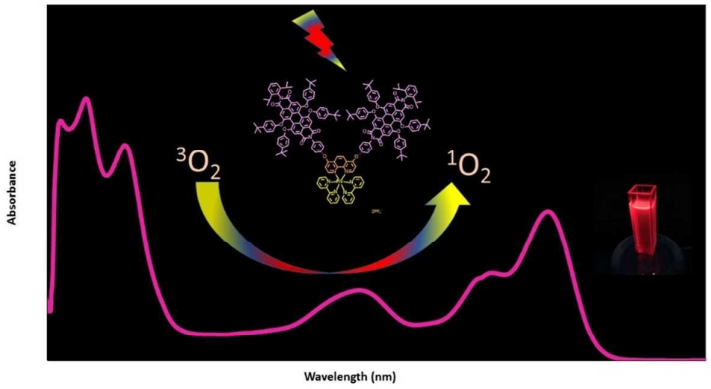

In this study, a novel photosensitizer having two perylenediimide and phenanthroline ruthenium (II) coordination moieties (**Ru-BP)** has been developed for photodynamic therapy (PDT) of cancer cells.